Aalborg Universitet

AALBORG UNIVERSITY
DENMARK

Disturbance Control of the Hydraulic Brake in a Wind Turbine

Jepsen, Frank ; Søborg, Anders ; Yang, Zhenyu

Disturbance Control of the Hydraulic Brake in a Wind Turbine

Frank Jepsen, Anders Søborg, and Zhenyu Yang

Department of Electronic Systems
Aalborg University, Esbjerg Campus
Niels Bohrs Vej 8, 6700 Esbjerg, Denmark.

Abstract—This paper discusses control of the brake torque from the mechanical disc brake in a wind turbine. Brake torque is determined by friction coefficient and clamp force; the latter is the main focus of this paper. Most mechanical disc brakes are actuated by hydraulics, which means that controlling caliper pressure is the key to controlling clamp force. A pressure controller is implemented on a laboratory-sized test system and uses a disturbance estimator to reject disturbances in order to track a reference curve. The estimator is capable of estimating both input equivalent disturbances and disturbances caused by brake disc irregularities. The controller can reject input equivalent disturbances and a strategy for cancelling the disturbance from the brake disc is proposed.

I. INTRODUCTION

The mechanical brake is one[1] of the two independent brake systems in a wind turbine. As a consequence of the gearing in the turbine, the mechanical brake is often placed on the high-speed shaft as this allows the brake system to be small as opposed to placing it on the low-speed shaft. This is shown in figure 1. The downside of this design is however, that the gearbox has to be able to handle a large amount of torque when the brake is applied.
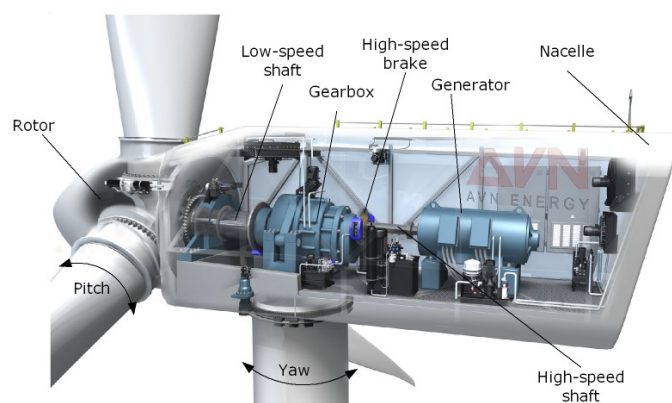

Fig. 1: Overview of drive train in a wind turbine [1]

Most brake systems in today's wind turbines supply the hydraulic brake caliper with maximum pressure when applied. Results in [2] show that such brake systems produce backlashes in the gearbox, that in the end may cause the fatigue load to be underestimated by current gearbox design methods.

---

[1]The other brake system is the aerodynamic brake, which uses the blades on the rotor to brake.

Furthermore, results from [3] show that when maximum brake torque is applied it excites oscillations in the rotor shaft, that have an amplitude nearly twice as high as the norminal shaft torque. Therefore, it is possible that the mechanical brake is the cause of a large amount of the gearbox failures. One such failure has been seen recently at Hornslet in Denmark, where a gearbox suffered a catastrophic failure caused by load from the mechanical brake system[4].

In recent years the term "soft brake" has been subject to great interest from companies such as Svendborg Brakes, General Electric and Nordex. All three companies have filed patents for "soft brake" systems as described in [5], [6], [7]. All three patents are concerned with reducing the excessive dynamic load peaks and vibrations during emergency stops. Comparing "soft brake" with the classic approach, where full pressure is applied, it is clear the soft brake is superior. However, "soft brake" still leave room for improvement as relatively large oscillations still occur – especially after the shaft has stopped [5].

This paper focuses on a **smart brake** system which has the objective of controlling the brake torque through precise control of the calipers clamp force. Since none of the "soft brake" systems directly control the force but depends on other factors such as rotational speed or time; controlling the brake torque is believed to further damp the vibrations during emergency stops. At this first development stage, the control design focused on controlling the hydraulic pressure in the brake caliper using a laboratory-sized hydraulic brake system. However, it was observed that disturbances made it hard to keep a constant pressure in the caliper. As a result, a disturbance estimator was used to assist the design of a controller that can track a reference curve. The estimator is able to estimate disturbances caused by brake disc irregularities and a strategy for cancelling out these disturbances is proposed.

The rest of the paper is organized in the following way: Section II describes the physical setup; Section III discusses the mathematical modeling and parameter identification of the hydraulic system; Section IV briefs the development and implementation of the disturbance estimator while section V describes the disturbance rejection scheme applied; and finally discussion and conclusion as found sections VI and VII.

II. Setup

In order to investigate how the brake torque can be controlled by the mechanical brake, a laboratory-sized setup consisting of a test rig and a hydraulic power pack has been constructed. As shown in 2, the torque from the rotor is represented by a motor which is connected to the brake disc and caliper through a single shaft.
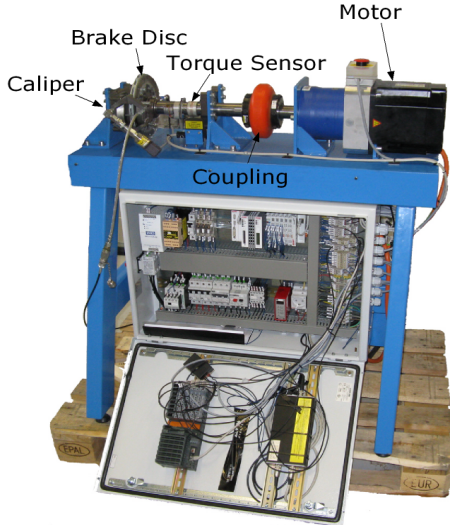

Fig. 2: The test rig

As the angle of twist in the shaft increases when the brake is applied, a set of wireless strain gauges are used to meassure the brake torque. In addition, two other sensors are also placed on the test rig; a tachometer to measure the angular velocity of the shaft and a IR temperature sensor to measure the temperature of the brake disc.

The hydraulic power pack, which provides oil to the caliper, is divided into two subsystems; hydraulic control system and hydraulic power system. The purpose of the power system is to provide a contant pressure to the control system. The hydraulic control system is the part that actually controls the pressure in the caliper using a proportional pressure valve; as shown in figure 3. On the system there are two pressure sensors; one to measure the outlet pressure of the proportional pressure valve and one to meassure the pressure in the caliper.

III. Modelling and Identification

To model the hydraulic control system, a series of preliminary experiments was conducted. These tests served as on-hands experience with the system to insure that no important phenomenons was left out in the model and to see how the proportional valve would react to different input voltages; regarding rise time, steady state gain, overshoot and dead time. Also it was of great interest to know if the shaft rotation affects the hydraulic system.

A. Dynamic Response of the Proportional Valve

The first thing that was observed when experimenting with the valve was the fact that it is necessary to use $7V$ as a
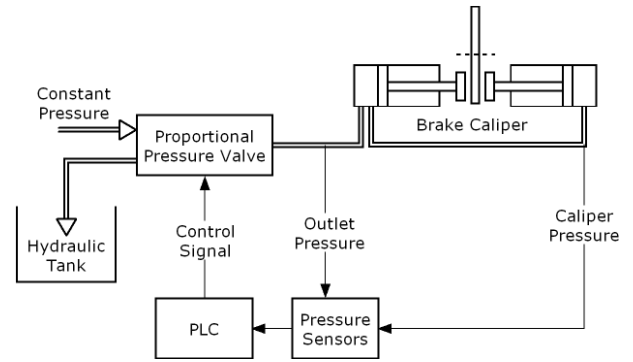

Fig. 3: The hydraulic control loop

virtual zero, because voltages below this limit did not have any effect on the outlet pressure. Figure 4 shows the measured step responses of the hydraulic system, when applying input steps of $8V$, $9V$, and $10V$ respectively.

From these steps it can be observed that the outlet pressure p_o has a rise time of approximately $0.05s$, a settling time between $0.2s$ and $0.3s$ and an overshoot of around $0.04MPa$. A dead time of about $0.01s$ to $0.02s$ was also observed. It seems that the hydraulic line and the caliper acts as a lowpass filter, where the settling time of caliper pressure p_c is approximately equal to the one of p_o.

The dynamic response when lowering the voltage from $8V$,$9V$, and $10V$ to $7V$ showed that both p_c and p_o settles in approximately $0.2s$ without any overshoot.

B. Effect of Brake Disc Irregularities

Brake disc irregularities is caused by variations in the contact surface between the pads and the disc on the micro level[8]. Three experiments was conducted to see the effect of brake disc irregularity; one at 0 rpm, one at 200 rpm, and one at 400 rpm. The rotational speed was kept constant using the servo motor. In each experiment the valve voltage was set to $8V$, $9V$, and $10V$ while measuring the hydraulic pressure. The measurements at 200 rpm is shown in figure 5.

The disturbance from the brake disc is periodic with a frequency close to the frequency of the shaft rotation and
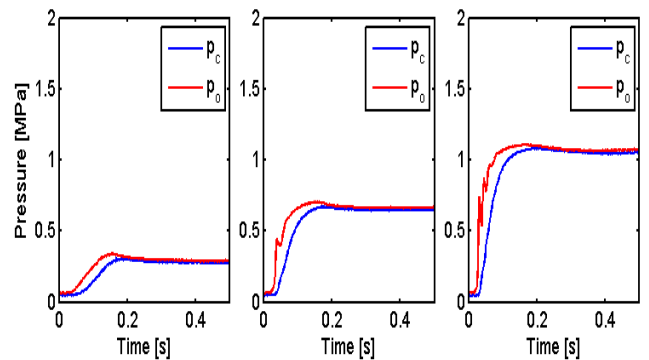

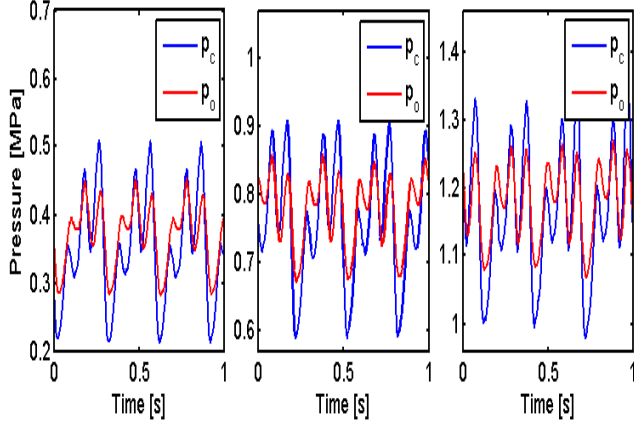Fig. 4: Measured step responses with input steps of $8V$, $9V$, and $10V$

Fig. 5: Pressure at $8V$, $9V$, and $10V$, and rotational speed at 200 rpm

as shown in the figure, it has a significant impact on the hydraulic pressure. At 200 rpm the disturbance affects the caliper pressure with an approximately constant value of about $\pm 0.15 Mpa$, whereas the disturbance effect at 400 rpm would depend slighty on the input voltage. To verify that the oscillations has a significant impact on the brake performance, the measured dynamic shaft torque from the experiments was also measured. It showed that in comparision with the motors maximum torque, of $147 Nm$, the oscillations in the shaft torque of $\pm 20 Nm$ where quite significant.

C. Overview of the Model

A mathematical model of the hydraulic system is developed to assist the design of a pressure controller. For this, a simple linear model with a constant input-equivalent disturbance and sinusoidal input to the caliper is proposed. The idea is to make a rough model and use real-time estimation of the disturbances to account for modelling errors and disturbance from the brake disc irregularities. A sketch of the model's structure is illustrated in figure 6 and is based on experience from the experiments described above.
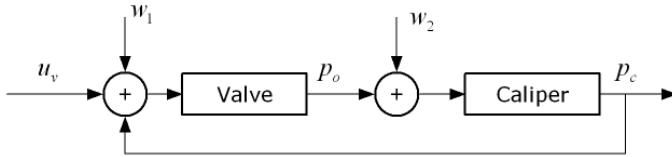

Fig. 6: Sketch of the model's structure

By looking at figure 4 and neglecting the overshoot in rising direction, the model from both valve voltage to outlet pressure and outlet pressure to caliper pressure can be seen as first order systems. From the sketch it can be seen that the model has the following inputs, outputs, and states:

- 2 states: outlet pressure and caliper pressure; p_o and p_c
- 1 output: caliper pressure; p_c
- 1 controllable input: valve voltage; u_v

- 2 uncontrollable inputs: constant disturbance and sinusoidal disturbance; w_1 and w_2

The differential equations describing the model can then be expressed as eq. (1) and (2), where k_{pc} is a constant related to the resistance of the hydraulic line and the volume of the caliper, k_{po} is related to the speed of the internal regulation in the valve while k_{dc} is the steady state gain.

$$\dot{p}_c = k_{pc} \cdot (p_o + w_2 - p_c) \tag{1}$$
$$\dot{p}_o = k_{po} \cdot (k_{dc} \cdot (u + w_1) - p_o) + k_{pc} \cdot (p_c - p_o) \tag{2}$$

The model for the disturbance is based on eq. (3) and (4), which describe the two disturbance signals, where the constant ω_0 is the frequency of the disturbance, that in turn is related to the brake disc irregularities. To use this model, the rotational speed has to be constant; however, by extending the model to a nonlinear case where ω_0 is a function of rotational speed, this requirement could be dropped.

$$\dot{w}_1 = 0 \tag{3}$$
$$\ddot{w}_2 = -\omega_0{}^2 \cdot w_2 \tag{4}$$

D. Plant Model

The state vector X is defined as

$$X \equiv \begin{bmatrix} x1 \\ x2 \end{bmatrix} = \begin{bmatrix} p_c \\ p_o \end{bmatrix}$$

to form a standard state space system for the plant of the form:

$$\dot{X} = A \cdot X + B_u \cdot u + B_w \cdot w \tag{5}$$
$$y = C \cdot X \tag{6}$$

where,

$$u \equiv u_v - 7V \quad, \quad w \equiv \begin{bmatrix} w_1 \\ w_2 \end{bmatrix} \quad, \quad y \equiv \begin{bmatrix} y_1 \\ y_2 \end{bmatrix} = \begin{bmatrix} p_c \\ p_o \end{bmatrix}$$

Using eq. (1) and (2) yields the following system matrices:

$$A = \begin{bmatrix} -k_{pc} & k_{pc} \\ k_{pc} & -k_{pc} - k_{po} \end{bmatrix} \qquad B_u = \begin{bmatrix} 0 \\ k_{po} \cdot k_{dc} \end{bmatrix}$$

$$B_w = \begin{bmatrix} 0 & k_{pc} \\ k_{po} \cdot k_{dc} & 0 \end{bmatrix} \qquad C = \begin{bmatrix} 1 & 0 \\ 0 & 1 \end{bmatrix}$$

By adding a delay of $0.02s$ and tuning the coefficients to match the real response, the following values are found:

$$k_{pc} = 40 \quad, \quad k_{po} = 70 \quad, \quad k_{dc} = 0.35$$

A simulation of the model with no disturbance, but including the $0.02s$ delay is seen in figure 7. Here it is compared to the real response of the hydraulic system and it is seen that
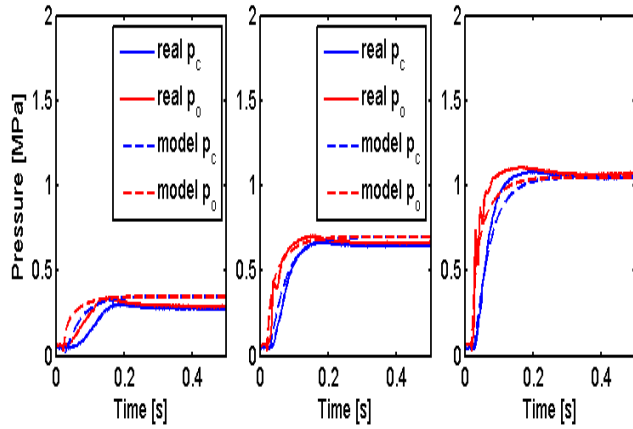
Fig. 7: Comparison of real hydraulic system and model with $0.02s$ delay

Fig. 8: Comparison of simulated step responses using different w_2 and input u

the model resembles the system somewhat, but especially the overshoot is missing.

The missing overshoot in the model is however a deliberate choice, since there is no overshoot when applying a step in negative direction. The model is considered satisfactory seen in relation to its simplicity. However, there are features not captured by the model, these are: nonlinear steady-state gain; ripples on p_o during a step in position direction; second order behaviour of p_o during a step in positive direction; different dead-time at step responses in both positive and negative direction.

In order to produce the simulation shown in figure 7, the valve voltage was set to match the experiment and the disturbance input was set to zero. This means that a more realistic disturbance signal should be constructed, if the model should fit perfectly to the experimental data. w_1 can be used to compensate for the input equivalent model error, while w_2 can be used to compensate for errors that enters the model through p_c.

Figure 8 shows step responses of the model at different valve voltages. A sinusiodal disturbance signal is applied through w_2, where the amplitude is constant but the frequency in the first plot corresponds to a rotational speed of 200 rpm and in the two last plots it corresponds to 400 rpm. It is seen that the response of the model shows the same features as figure 5.

E. Disturbance Model

A model of the disturbance is made with the purpose of augmenting the plant model and estimate both the disturbance and the states, and thereby use a control algorithm for disturbance rejection.

The disturbance model has no input and it's structure is seen in the following equations:
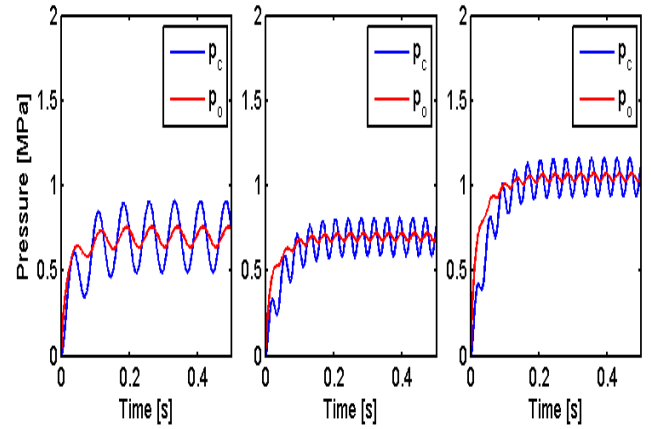
$$\dot{X}_d = A_d \cdot X_d$$
$$w = C_d \cdot X_d$$

where,

$$X_d \equiv \begin{bmatrix} x3 \\ x4 \\ x5 \end{bmatrix} = \begin{bmatrix} w_1 \\ w_2 \\ \dot{w}_2 \end{bmatrix} \quad , \quad w \equiv \begin{bmatrix} w_1 \\ w_2 \end{bmatrix}$$

Eq. (3) and (4) describes w_1 as a constant disturbance and w_2 as a sinusdiodal disturbance with constant frequency and amplitude. These are used to form the system matrices of the disturbance model:

$$A_d = \begin{bmatrix} 0 & 0 & 0 \\ 0 & 0 & 1 \\ 0 & -\omega_0{}^2 & 0 \end{bmatrix} \quad , \quad C_d = \begin{bmatrix} 1 & 0 & 0 \\ 0 & 1 & 0 \end{bmatrix}$$

where ω_0 determines the frequency of w_2 and the initial conditions determine the amplitude of w_1 and w_2 respectively.

F. Augmented Model

The plant model is augmented with the disturbance with the purpose of using a disturbance rejection scheme, which will be described in section V.

The structure of the augmented model is seen in the following equations.

$$\begin{bmatrix} \dot{X} \\ \dot{X}_d \end{bmatrix} = \begin{bmatrix} A & B_w \cdot C_d \\ \mathbf{0} & A_d \end{bmatrix} \cdot \begin{bmatrix} X \\ X_d \end{bmatrix} + \begin{bmatrix} B_u \\ \mathbf{0} \end{bmatrix} \cdot u$$
$$y = \begin{bmatrix} C & \mathbf{0} \end{bmatrix} \cdot \begin{bmatrix} X \\ X_d \end{bmatrix}$$

This can be written as

$$\dot{X}_a = A_a \cdot X_a + B_a \cdot u$$
$$y = C_a \cdot X_a$$

where,

$$X_a \equiv \begin{bmatrix} x_1 \\ x_2 \\ x_3 \\ x_4 \\ x_5 \end{bmatrix} = \begin{bmatrix} p_c \\ p_o \\ w_1 \\ w_2 \\ \dot{w}_2 \end{bmatrix}$$

and

$$A_a = \begin{bmatrix} -k_{pc} & k_{pc} & 0 & k_{pc} & 0 \\ k_{pc} & -k_{pc} - k_{po} & k_{po} \cdot k_{dc} & 0 & 0 \\ 0 & 0 & 0 & 0 & 0 \\ 0 & 0 & 0 & 0 & 1 \\ 0 & 0 & 0 & -\omega_0{}^2 & 0 \end{bmatrix}$$

$$B_a = \begin{bmatrix} 0 \\ k_{po} \cdot k_{dc} \\ 0 \\ 0 \\ 0 \end{bmatrix} \quad , \quad C_a = \begin{bmatrix} 1 & 0 & 0 & 0 & 0 \\ 0 & 1 & 0 & 0 & 0 \end{bmatrix}$$

IV. DISTURBANCE ESTIMATOR

A disturbance estimator is designed to estimate w_1 and w_2 in the augmented model. For that purpose, a current estimator with equations (7) and (8) is used. $\bar{x}$ is the predicted states and $\hat{x}$ is the current estimate, while Φ, Γ, and H are the discretized versions of A_a, B_a, and C_a respectively.

$$\bar{x}[k] = \Phi \cdot \hat{x}[k-1] + \Gamma \cdot u[k-1] \tag{7}$$

$$\hat{x}[k] = \bar{x}[k] + L_c \cdot (y[k] - H \cdot \bar{x}[k]) \tag{8}$$

The estimator gain L_c is designed by pole placement and the two dominant poles are:

$$z = 0.8673 \pm 0.05554i$$

Figure 9 shows the estimated disturbances together with the measured pressure for a data set where the valve voltage is $10V$ and the rotational speed is 400 rpm.

A comparison of the measured pressure and the model described in eq. (5) and (6), is made by using the estimated disturbances (shown in figure 9) as input signals to the model. In the comparison, which is shown in figure 10, it is seen that a good estimation of the disturbance is obtained, since the output of the model fits the experimental data.

V. DISTURBANCE REJECTION

A controller with disturbance rejection of w_1 is designed, using the scheme shown in figure 11. The estimator described in the previous section is used together with an LQR controller.

K is calculated by disregarding B_w, using eq. (5) and (6), and by using the following weightings:

$$R = 0.1 \quad , \quad Q = \begin{bmatrix} 5 & 0 \\ 0 & 1 \end{bmatrix}$$
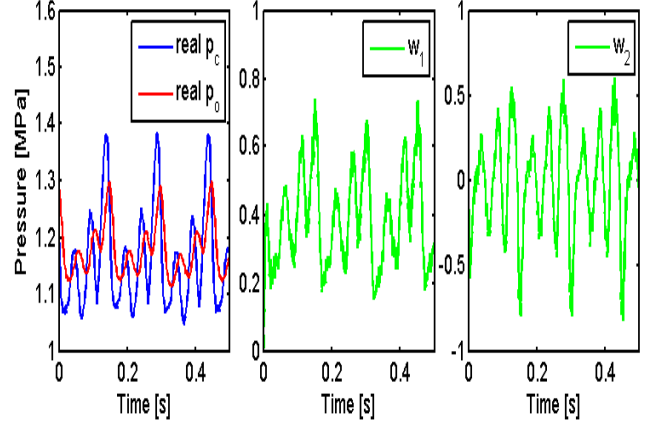

Fig. 9: Estimation of disturbance signals during constant speed and constant valve voltage.
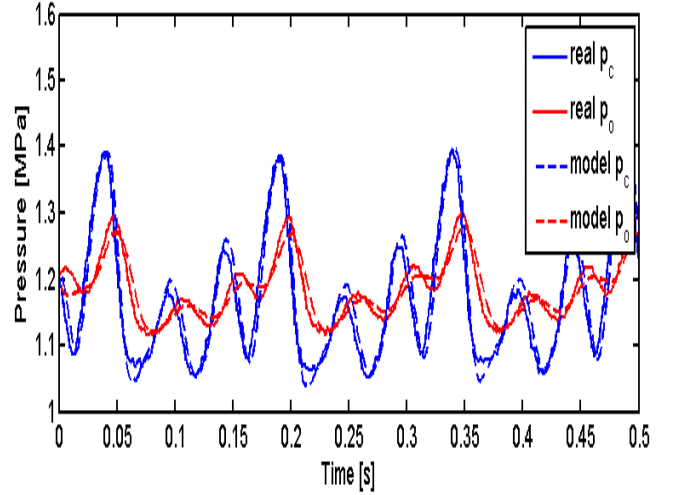

Fig. 10: Comparison of experimental data and simulation, where the estimated disturbance is used as input for the simulation model.

It was found necessary to apply a low-pass filter to the estimation of w_1, before using it for control purposes, since it would induce oscillations in the control loop otherwise. A forth order Buttorworth filter with a cutoff frequency of $3Hz$ was found suitable.

On figure 12 it is seen that the caliper pressure tracks the reference in an acceptable maner; this is also what was expected, since there should be no disturbance from w_2 when the speed is 0 rpm and the estimation of w_1 compensates for modelling errors. However, in figure 13, it is clear that the disturbance from w_2 affects the performance of the controller and that this disturbance is not cancelled by the applied control scheme.
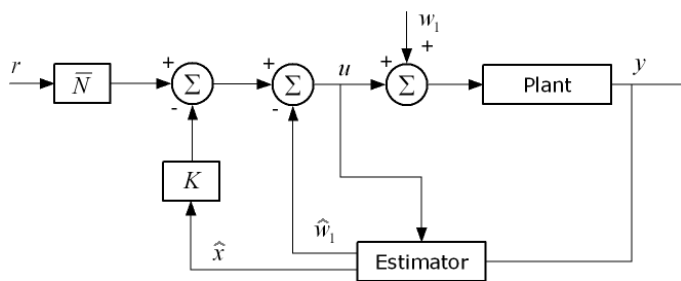
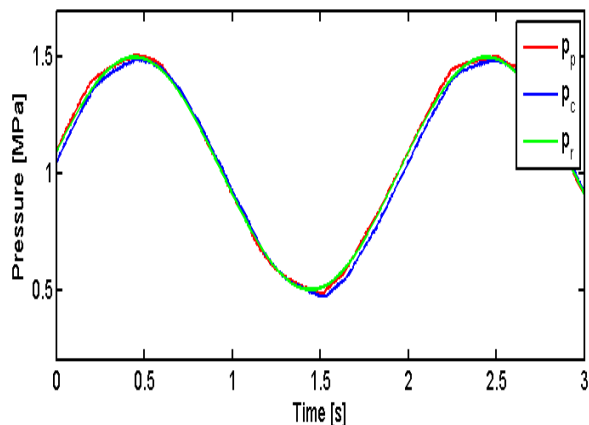Fig. 11: Block diagram for input disturbance rejection [9]

Fig. 12: Performance of controller when speed is 0 rpm

Fig. 13: Performance of controller when speed is 400 rpm

VI. DISCUSSION

It is not possible to rewrite the disturbance from w_2 to be input equivalent. Therefore, the control scheme applied in section V cannot be used to cancel that disturbance. However, by improving the disturbance model, it is believed that the disturbance from w_2 can be integrated into the plant model and used when designing the controller. The work presented in this paper points toward making the frequency of w_2 dependent on the shaft speed and creating an amplitude modulation which is dependent on the brake pad' position on the disc.

VII. CONCLUSION

Through experiments it has been found that the disturbance from the brake disc/caliper to the hydraulic pressure is dependent on the shaft's speed and the position of the brake pads on the disc. An estimator has been designed, which is proven succesfull in estimating the amplitude of this disturbance. The estimator uses a linear model, which is known to have some uncertainties that can be described as input equivalent disturbances. A disturbance rejection scheme has been applied to show that it is possible to reject the input equivalent disturbance. Future research should focus on obtaining a frequency and amplitude model of the disturbance from the brake disc/caliper, which can be used when designing a controller that controls the caliper pressure and cancels out disturbance from the brake disc/caliper.
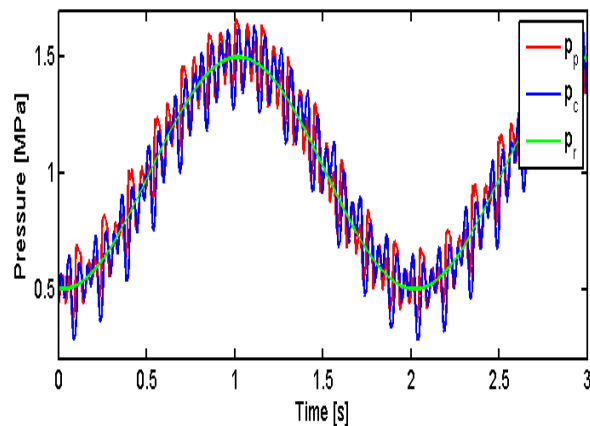
REFERENCES

[1] AVN Energy A/S. *Overview of nacelle internals*
[2] A. Heege, J. Betran, and Y. Radovcic. *Fatigue Load Computation of Wind Turbine Gearboxes by Coupled Finite Element, Multi-body System and Aerodynamic Analysis*. Wind Energy 2007; 10(5): 395-413.
[3] B. Schlecht and S. Gutt. *Multibody-System-Simulation of Drive Trains of Wind Turbines*. Fifth World Congress on Computational Mechanics. 2002.
[4] Risø DTU. *Endelig rapport for Risø DTU's undersøgelse af møllehavarier på Vestas møller den 22. og 23. februar 2008*. Technical report. 2008.
[5] Svendborg Brakes A/S. *Hydraulic Braking System*. US6254197B1. 2001.
[6] General Electric Company. *Hydraulic Brake System for a Wind Energy Plant*. US7357462B2. 2008.
[7] Nordex Energy GmbH. *Wind Energy Plant with a Hydraulically Actuated Rotor Brake*. US7494193B2. 2009.
[8] Mikael Eriksson. *Friction and Contact Phenomena of Disc Brakes Related to Squeal*. Uppsala University, PhD thesis. 2000
[9] G. F. Franklin, J.D. Powell, and M.Workman *Digital Control of Dynamic Systems*. Pearson Education. 2006.